

Synthesis and Characterization of Brush Copolymers Based on Methoxy Poly(ethylene glycol) and Poly(ϵ -caprolactone)

Madhab Prasad Bajgai,¹ Santosh Aryal,² Daman Chandra Parajuli,¹ Myung-Seob Khil,³ Duck Rae Lee,³ Hak Yong Kim³

¹Department of Bionanosystem Engineering, Chonbuk National University, Jeonju 561-756, Republic of Korea

²Department of Bionanosystem Engineering, Centers for Healthcare Technology Development, Chonbuk National University, Jeonju 561-756, Republic of Korea

³Department of Textile Engineering, Chonbuk National University, Jeonju 561-756, Republic of Korea

Received 6 March 2008; accepted 21 July 2008

DOI 10.1002/app.29168

Published online 30 October 2008 in Wiley InterScience (www.interscience.wiley.com).

ABSTRACT: Brush copolymers composed of methoxy poly(ethylene glycol) (MPEG) and poly(ϵ -caprolactone) (PCL) have been synthesized by the ring-opening polymerization of ϵ -caprolactone initiated by hydroxyl function of thermally esterified MPEG-citrate in presence of stannous octoate. Citric acid (CA) acts as spacer between brush-like MPEG and the long chain of PCL. Existence of hydrophobic domains as cores of the micelles were characterized by ¹H NMR spectroscopy and further confirmed with fluorescence technique using pyrene as a probe. Critical micelle concentration (CMC) of the synthesized copolymer decreased from 0.019 to 0.0031 mg/mL on increasing the fraction of PCL. Along with the physicochemical study, the brush copolymers were explored for the preparation of nanoparticles by nano-

precipitation technique. The morphology and geometry of micelles were investigated by using DLS, AFM, and TEM. Hydrodynamic dimensions of micelles were around 118 and 178 nm with the core size of 8–10 nm, which further aggregated to form secondary micelle of 60–90 nm. Such assembled polymeric micelles with its flexible dendritic MPEG corona could hold a promise for the immobilization (encapsulation) of hydrophobic drugs and subsequently promote sustained release so that it can be a good vehicle for anti-cancer drug deliverance. © 2008 Wiley Periodicals, Inc. *J Appl Polym Sci* 111: 1540–1548, 2009

Key words: biodegradable; brush copolymers; esterification; polyesters; nanoparticles

INTRODUCTION

The concept of block copolymer synthesis started in 1956 when Szwarc discovered living anionic polymerization of styrene.^{1–5} These days amphiphilic linear block copolymers are serving as new nanosphere systems that would offer versatility in the choice of polymer core to facilitate controlled entrapment, degradation, and release of a variety of bioactive materials.⁶

In comparison with the linear block polymers, dendrimers have much more accurately controlled structures, with a globular shape.^{7–9} The well-defined geometry, size monodispersity, and control-

lable surface functionalities of dendrimers make them excellent candidates for evaluation as drug carriers.¹⁰ Such dendrimers are used as potential drug-delivery agents either by physical entrapment or through covalent attachment to afford dendrimers drug conjugates.¹¹

Biodegradable aliphatic polyesters, including poly(ϵ -caprolactone) (PCL), poly(lactic acid) (PLA), poly(*p*-dioxanone) (PPDO), and poly(glycolic acid) (PGA) have received great research interest for their environmental, medical, and pharmaceutical applications.^{12,13} Although PLA, PGA, and PPDO are biodegradable and biocompatible synthetic polymers, faster degradation of PGA, lactic acid deposition after degradation by PLA, and irregular degradation of PPDO make them secondary in choice than PCL in long-term medical applications. Among the polyesters, PCL degrades most slowly due to the five hydrophobic $-\text{CH}_2$ moieties in its monomer. PCL also possesses strong mechanical properties similar to those of polyolefin.^{14–16}

Nevertheless, long-term *in vivo* use of PCL for drug delivery causes harmful effects to tissue, mainly due to high crystallinity.⁷ On the other hand,

Correspondence to: H. Y. Kim (khy@chonbuk.ac.kr).

Contract grant sponsor: Korea Research Foundation; contract grant number: KRF2007-211-D00032 (project number 10028211).

Contract grant sponsors: The Ministry of Commerce, Industry and Energy Department, Center for Healthcare Technology Development.

PEG presents outstanding properties, e.g., hydrophilicity, solubility in water and in organic solvents, nontoxicity, and absence of antigenicity.¹⁵ Hence, if ϵ -caprolactone (ϵ -CL) is copolymerized with PEG, its biodegradability and mechanical properties can be improved.^{17,18} In addition, the physiochemical properties of PCL can be changed by PEG.¹⁹

Several groups have studied the PEGylation of synthetic polymers. For instance, Lu et al. found that thermal properties of PEG-PCL block copolymers were influenced by the PEG weight fractions.²⁰ Shabat et al. observed significant improvement in hydrophilicity in MPEG/PLA copolymer than PLA.⁶ Kim et al. found higher release of bovine serum with synthesized MPEG-PCL than that of physical blend.⁷ Although various studies on PEG- and PCL-based copolymers have been made, physiochemical study of MPEG-citric acid (CA)-PCL has not been reported yet.

No doubt, PEG-PCL diblock copolymers were found to be useful for the preparation of nanoparticles and drug release. For site-specific drug administration, drug particles uptake by macrophages can be greatly reduced by brush like conformation.²¹ In addition, such configuration may influence both the release profile of the incorporated drug and the blood circulation time of the nanoparticles.^{7,21} Tricarboxylic acid (CA) has been chosen to act as a spacer between PCL and PEG, so as the number of PEG chain branches from a PCL chain end to provide nanoparticles rich in "external" PEG environment. Also, CA is cheap and readily available nontoxic metabolic product of the body.²² The current study of brush-like MPEG-PCL copolymer, in which the core is connected to MPEG through a hydroxyl function of CA, may be used to form nanoparticles for drug-delivery applications.²³

Depending on the molecular geometry, colloidal self-assemblies of amphiphilic copolymers in aqueous dispersion can result up to three types of micelles: primary (smaller than 50 nm), secondary (larger than 50 nm), and crew-cut micelles (large up to 1200 nm), formed by successive aggregation.²⁴ Micelles, smaller than 1 μ m, circulate in blood stream without immobilization at capillaries and permeate into the target cells through blood vessels.¹⁴ It is worthwhile to mention that the hydrophilic corona, mostly composed of MPEG and CA moiety, endowed the polymeric micelles from possible nonspecific uptake by RES. Accordingly, long systemic circulation can be achieved by introducing the MPEG component into polymeric micelle systems that complement a brush-type structure with multifunctionality of CA.⁷ Such micelles prepared from the MPEG-CA-PCL (hence after referred as MPCL) can be a milestone in drug-delivery system.¹³ Herein, we describe the synthesis, characterization,

and physiochemical study of a novel biodegradable MPCL-brush copolymers, which is potential for the use in drug-delivery system, in particular, delivery of anticancer drugs.

EXPERIMENTAL

Materials

ϵ -CL (Aldrich, St. Louis, MO) was dried over CaH₂ and distilled under reduced pressure just before use. MPEG (Aldrich, USA), with number average molecular weights of 5000 and 550 daltons, were purified by extraction with diethyl ether followed by drying through azeotropic distillation in toluene. CA (Aldrich, USA) was dried in vacuum for 24 h just before use. Stannous octoate [Sn (Oct)₂], dicyclohexylcarbodiimide (DCC), and 4-(dimethylamino) pyridine (DMAP) were purchased from Aldrich, USA, and used as received. All other chemicals were analytical pure grade and used as received.

MPCL synthesis

MPCL has been prepared through esterification of CA followed by ring opening polymerization (ROP). Esterification has been carried out by two methods. In one method, MPEG (M_n 5000, 0.2 mmol, 1.0 g), CA (0.11 mmol, 23 mg), DCC (0.2 mmol, 39 mg), and DMAP (4 mg) were dissolved and kept under stirring at room temperature in dichloromethane/tetrahydrofuran (1 : 1 v/v) for 4 days under dry conditions, as studied earlier.⁶ The sediment was filtered and the filtrate was added to mixture of 100 mL ether/petroleum ether (50 : 50) to obtain trimethoxy poly(ethylene glycol) (MPEG) citrate.

In the next method, esterification has been done without the use of catalyst as described in earlier literatures.^{7,25} Briefly, MPEG 550 and CA (molar ratio of MPEG/CA = 1 : 3, 1 : 4, 1 : 5, 1 : 9, and 9 : 10) were added to a 250 mL three-necked flask fitted with an inlet and outlet adaptor. The mixture was melted under nitrogen by stirring at 155°C over silicon oil bath. The mixture was stirred for 24 h at 130°C to obtain MPEG citrate. For the removal of unreacted MPEG, MPEG citrate was dissolved in acetone and then precipitated in distilled water, washed with a large amount of water for several times, filtered, and followed by drying in a vacuum oven for 48 h. MPEG citrate obtained by both the above methods has been employed for subsequent ROP of ϵ -CL in the presence of hydroxyl group of MPEG citrate as macroinitiator and stannous octoate as a catalyst, similar as earlier study.^{7,25} Shortly, MPEG citrate and ϵ -CL (molar ratio of ϵ -CL to MPEG citrate is equal to 400) were dissolved in dry

toluene (50 mL) under nitrogen environment. Stannous octoate (0.039 mol/L, 0.045 mL) was added in the reaction mixture and maintained at 130°C for an additional 12 h. The solvent was evaporated under nitrogen to obtain a solid product, which was purified by dissolving in MC and precipitating in diethyl ether. The yield so obtained was vacuum dried before characterization. The polymer obtained with earlier method (MPEG of M_n 5000) is referred as MPCL1 and latter were referred as MPCL3, MPCL4, MPCL5, MPCL9, and MPCL10, respectively, in this manuscript.

Preparation of MPCL nanoparticles

Nanoparticles were prepared in triple distilled water using cosolvent evaporation nanoprecipitation technique. MPCL (10 mg) was dissolved in acetonitrile (1.0 mL) and dropped into 10 mL of triple distilled water under moderate stirring (50 rpm) at room temperature. The organic phase was allowed to evaporate under reduced pressure until the final volume of the aqueous suspension was reduced to 10 mL. Finally, the suspension was filtered by a microfilter with 0.2 μm pore size to remove any polymer aggregates. Further to measure the physiological stability, the particles were prepared in phosphate buffered saline at pH 7.4.

Polymer characterization

^1H NMR spectra of the samples were recorded by JNM-Ex 400 FT-NMR spectrometer (JEOL, Japan), operating at 400 MHz; 6% (^1H) (w/v) sample solution in CDCl_3 and dimethyl sulfoxide- d_6 , using tetramethylsilane (TMS) as an internal reference. Fourier-transform infrared (FT-IR) spectra were recorded with KBr pellets using an ABB Bomen MB100 Spectrometer (Bomen, Canada). The molecular weight and molecular weight distributions were measured by gel permeation chromatography (GPC) and the measurements were made via a Waters 150C (Polymer Laboratories, England) using chloroform as a mobile phase at the flow rate of 1.0 mL/min. Wide-Angle X-ray Diffraction (WAXD) profiles of these copolymers were measured at room temperature on a Rigaku D/Max-Ra X-ray diffractometer employing Ni filtered $\text{Cu K}\alpha$ radiation (30 kV, 50 mA, 1.5418 Å) at room temperature. The scanning rate was 0.04°/s. Thermogravimetric analysis (TGA) was carried on Perkin-Elmer TGA 6 thermogravimetric analyzer (Perkin-Elmer, USA) equipment under a nitrogen atmosphere with a heating rate of 10°C/min in the range of 25–600°C. Thermal property of polymer was measured by a DSC Q100 V 7.3 build 249 (Perkin-Elmer, USA) thermal analysis system. Samples were first heated from –9 to 160°C with a heating rate

of 10°C/min under nitrogen atmosphere and held for 5 min to remove the thermal history, then cooled to –9°C at 10°C/min, and finally heated to 160°C.

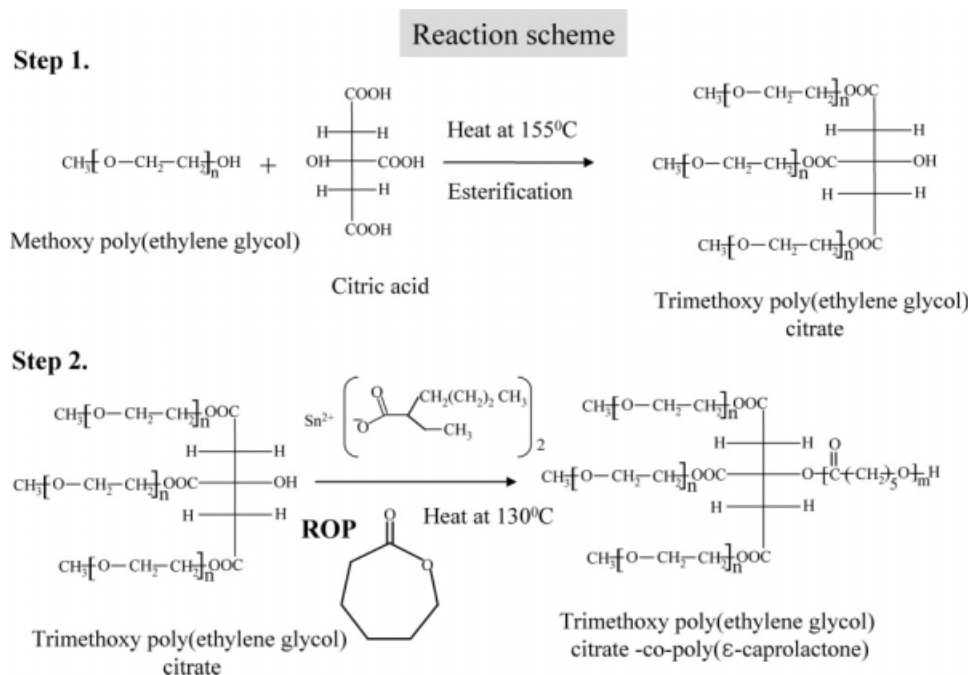
Nanoparticles characterization

Critical micelle concentration (CMC) of the polymeric nanoparticles was measured by steady state pyrene fluorescence method. Excitation spectra ($\lambda_{\text{em}} = 390 \text{ nm}$) of pyrene were measured at various polymer concentrations using F-200 fluorescence spectrometer 2510221-07 (Hitachi Co., Japan). Concentrations of polymer and pyrene were in the range of 1×10^{-4} to 1 mg/mL and $6 \times 10^{-7} \text{ M}$ in phosphate buffer (pH 7.4), respectively. CMC value of the polymeric nanoparticles was determined using intensity ratio of band 330 to 328 nm of pyrene in excitation spectra. The intensity ratio of I_{333}/I_{328} against polymer concentration ($\log c$) in pyrene excitation spectra was plotted. Size and surface morphology of the polymeric nanoparticles were observed by AFM nanoscope IV multimode (Digital Instrument, MicroMash Co., USA) in tapping mode using Si cantilever with a spring constant of 305 N/m and a resonance frequency of 75 kHz. Scanning was performed at scan speed of 1.85 Hz. Samples for AFM observations were prepared as a drop-coated film on the argon dried Si (111) wafers. Furthermore, morphological examination of the copolymer micelles was performed using a H7650 transmission electron microscope (Bio-TEM, Hitachi Co., Japan). A drop of MPCL copolymer aqueous solution (1 mg/mL) was dropped into a 400 mesh copper grid coated with carbon and was stained with phosphotungstic acid. The sample was dried before transmission electron microscopy (TEM) observation. Average particle size and size distribution were determined by dynamic light scattering method by ζ -potential and particle size Analyzer (Malvern System 4700 instrument CO., UK) equipped with vertically polarized light supplied by argon ion laser (Cryonics) operated at 20 mW. All experiments were performed at room temperature (25°C) of measuring angle 90° to the incident beam. Potential of the nanoparticles was determined by electrophoretic light scattering (ELS) measurement (ELS 8000/6000, Otsuka Electronics Co., Japan) at 25°C with a measuring angle of 20° when compared to the incident beam. Before analysis, samples were sonicated in an ultrasonicator bath for 1 min.

RESULTS AND DISCUSSION

Synthesis and characterization of MPCL

MPCL brush copolymers were synthesized initially by esterification of CA with MPEG and subsequent



Scheme 1 Reaction scheme for the synthesis of MPCL brush like copolymers. Step 1 represents the reaction scheme for activator free esterification and Step 2 is the reaction scheme for ROP and for the formation of brush like MPCL.

ROP of ϵ -CL by the available hydroxyl group of ester as a macroinitiator in presence of stannous octoate (Scheme 1). Generally, PCL homopolymer is a hydrophobic and semicrystalline in nature, contributing to a long degradation period (about 2 years) *in vivo*.²⁴ The introduction of MPEG citrate into a PCL chain not only improves the hydrophilicity and reduces the degradation time but also increase surface area due to brush-like conformation, thereby retain longer time in the blood and provide larger space for introducing materials/drugs. It is obvious to think that tri-MPEG citrate can result only by binding three equivalents of MPEG with one equivalent of CA, but due to steric hindrance the same is not obtained easily.⁷ Smaller the molecular weight of MPEG lesser is the hindrance and subsequently higher is the probability of esterification. In the cur-

rent experiment, we used different molar ratios of MPEG to CA and obtained highest binding with the ratio 9 : 10 (MPCL10) (Table I). The binding of three carboxylic acid groups with MPEG 550 is governed by the favorable ratio so as having lesser hindrance. Synthesized polymer was observed by bromophenol test to confirm the absence of carboxylic acid in the polymer.⁶ Subsequent ROP of ϵ -CL was carried out with these citrate esters in toluene solution at temperature 130°C for 24 h. The molar feed ratio and the obtained molecular weight of the different polymers have been mentioned in the Table II. We found the highest molecular weight with MPCL10 (M_w : 39,600 Dalton, GPC).

Again, the different behavior of polymerization among MPEG-citrates may be due to free carboxylic acid groups remaining in them. Such carboxylic acid

TABLE I
Characterization of MPEG Citrate Prepared by Various Methods

Sample	Molecular weight of MPEG (M_n)	Feed ratio of MPEG to citric acid (molar ratio)	Activator used for esterification	Molecular weight of MPEG citrate obtained	
				M_w	M_n
MPCL1	5000	1 : 3	DMAP/DCC	9250	7200
MPCL3	550	1 : 3	N/A	1290	1060
MPCL4	550	1 : 4	N/A	1250	1120
MPCL5	550	1 : 5	N/A	1120	1000
MPCL9	550	1 : 9	N/A	1130	950
MPCL10	550	9 : 10	N/A	1600	810

N/A, not applicable.

TABLE II
Physiochemical Properties of MPCL Brush Copolymers

Sample	Molar ratio of OH/ ϵ -CL	Molecular weight of MPCL (M_w) by GPC	PDI	Molecular weight of MPCL (M_n) by $^1\text{H NMR}$	DP_{PCL}	Mean diameter of micelle \pm SD by DLS (nm)	CMC \pm SD (mg/L)
MPCL1	400	15,500	1.6	9333	19	178 \pm 44	19 \pm 2.3
MPCL3	400	12,000	1.8	4996	35	165 \pm 35	6.3 \pm 1.7
MPCL4	400	16,100	1.7	5584	39	133 \pm 40	5.1 \pm 0.9
MPCL5	400	15,700	1.8	7123	54	130 \pm 20	5.7 \pm 1
MPCL9	400	35,400	2.4	13,911	114	222 \pm 29	4.25 \pm 0.9
MPCL10	400	39,600	1.9	16,945	138	118 \pm 22	3.1 \pm 0.6

SD, standard deviation.

groups may lead to esterification, which subsequently hinder ROP. Although all the MPEG-citrates (MPEG1-MPEG10) are similar compounds, MPEG10-citrate (M_w : 1600 daltons) has not free carboxylic acid group within it. In such cases, ROP favors longer PCL chain in MPCL10 during polymerization. This is the reason that polymerization behavior is different among the MPEG-citrates.

Figure 1 shows FT-IR spectra of MPEG, MPEG citrate, and MPCL10 copolymer. The strong peak of C=O stretch at 1734 cm^{-1} confirms the formation of ester bond with carboxylic moiety of CA. As the stretching is more intense in MPCL10 than MPEG citrate, it supports ROP of ϵ -CL. Further the distinguished peak at 720 cm^{-1} (methylene bending, when more than four $-\text{CH}_2$ groups are at linear conformation, PCL) is significant in favor of MPCL10. The distinct stretch of $-\text{OH}$ group at 3460 cm^{-1} indicates that the hydroxyl groups are hydrogen bonded.²² There is a broad band due to the inclusion of C-H stretching vibration at 2865 cm^{-1} of $-\text{CH}_2$ from MPEG together with methylene C-H stretching at 2943 cm^{-1} of PCL chain.²⁶ Also, the

bands at 1285 , 1240 , and 1190 cm^{-1} (C-O stretching of PCL and MPEG) and 1110 cm^{-1} (C-O-C, asymmetrical stretching vibration of ether links of MPEG) exhibit wider region. The absence of peak at 772 cm^{-1} suggests the absence of crystalline PCL in the polymer. Similarly, the disappearance of the peak at 1650 cm^{-1} (carbonyl C=O stretching vibration for carboxylic acid of CA) supports the absence free carboxylic groups in our synthesized polymer.

The WAXD results (Figure not shown) MPCL exhibited only two major peaks at (2θ) about 21.3 and 23.5° , which corresponded to the characteristic PCL crystalline peaks.²⁵ Although, the crystallinity of the polymer has been increased by increasing the PCL content in the polymer, but it was lesser than pure PCL.

The $^1\text{H NMR}$ spectrum of the MPCL10 copolymer is illustrated in Figure 2. $^1\text{H NMR}$ (CDCl_3 , TMS): 3.27 (1, s, $-\text{OCH}_3$ in MPEG end), 3.6 (3, s, $-\text{OCH}_2$ in MPEG), 4.24 (4, t, COOCH_2 , methylene protons of MPEG), 4.06 (8, t, COOCH_2 , methylene protons of PCL), 2.31 (5, t, OCOCH_2 in PCL), 1.65 (6, m, $\text{OCOCH}_2\text{CH}_2\text{CH}_2\text{CH}_2\text{CH}_2$ in PCL), 1.39 (7, m, $\text{OCOCH}_2\text{CH}_2\text{CH}_2\text{CH}_2\text{CH}_2$ in PCL), 3.8 (9, t,

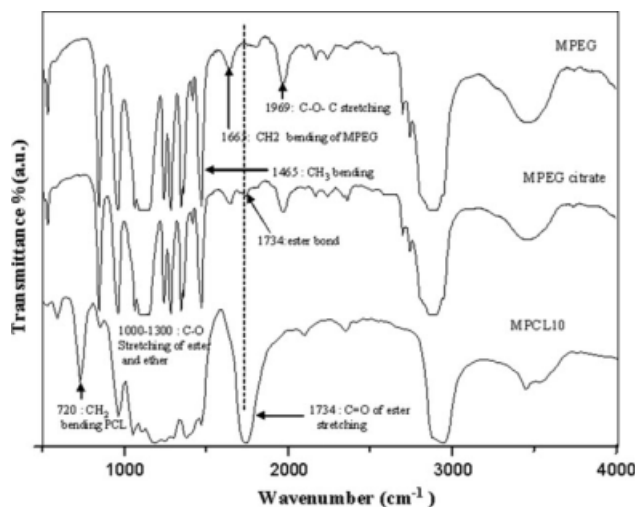


Figure 1 FT-IR spectra of MPEG, MPEG-citrate, and MPCL10 brush like copolymer.

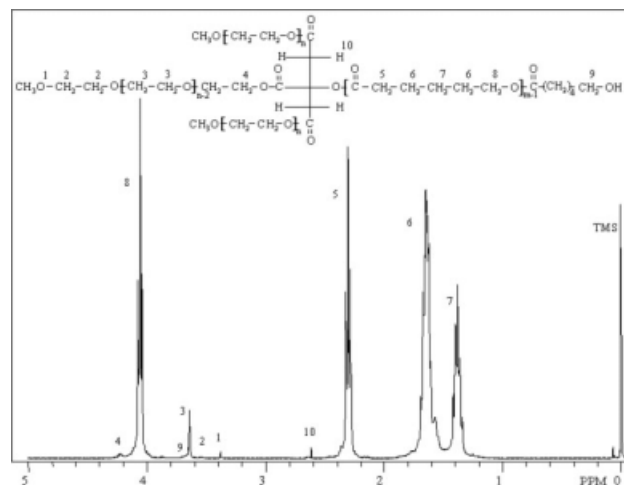


Figure 2 $^1\text{H NMR}$ (CDCl_3) spectrum of MPCL10 copolymer after precipitation into diethyl ether and vacuum dry.

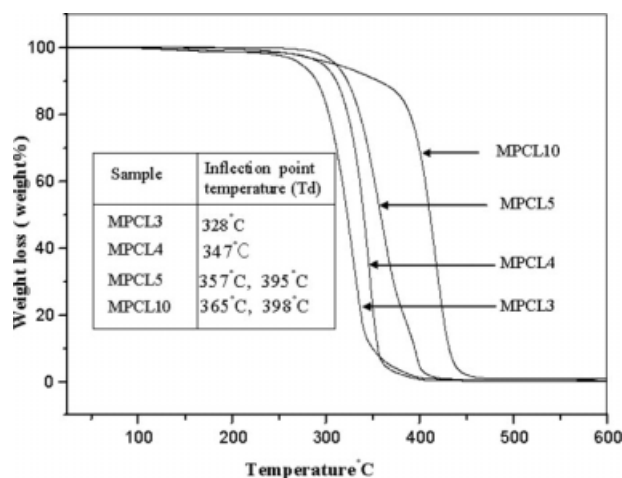


Figure 3 TG curves of MPCL brush like copolymers obtained by heating the samples from 25 to 600°C at 10°C/min under the steady flow of nitrogen.

OCOCH₂CH₂ CH₂CH₂CH₂ in PCL end), and 3.5 ppm (2, t, CH₃OCH₂, methylene proton at methoxy end in MPEG). Because the long-PEG arms shield unreacted hydroxyl groups, it is difficult to accurately predict the number of MPEG groups per unit.^{27,28} Therefore, the direct method using ¹H NMR to examine the protons from both MPEG and PCL was preferred. The integration area ratio of Signal 5 (δ 2.3, CH₂, PCL) to 1(δ 3.38, OCH₃, MPEG) has been used for the calculation of M_n by proton NMR as described in previous literature.^{7,19}

The number average molecular weights of MPCL and PCL block lengths in the polymer were calculated from the integration data of ¹H NMR spectra $\{[M_n \text{ of MPCL} = 114.1 (A_{\text{OCOCH}_2} \text{ of PCL} / A_{\text{OCH}_3} \text{ of MPEG})] + M_n \text{ of the MPEG citrate}\}$. Similarly, the degree of polymerization PCL (DP_{PCL}) has been calculated as: $DP_{\text{PCL}} = (M_n \text{ of MPCL} - M_n \text{ of the MPEG citrate}) / 114.1$. The results are summarized in Table II. The average molecular weight and polydispersity indexes were measured by GPC (Table II) using chloroform as solvent and monodisperse polystyrene as standards.

TGA is the best method for characterizing the copolymers.²⁹ Polymeric composition can be obtained by the qualitative characterization of degradation process illustrated by the inflection point temperature (T_d) and the weight loss percentage (ΔW). TG curve of the copolymer is portrayed in Figure 3. MPCL5 and MPCL10 showed two weight loss steps. The calculated T_d and ΔW values suggested that the first weight loss step was due to the PCL segment and the second one due to the MPEG citrate unit. DSC results (data not shown) showed that T_m and T_c of the polymers linearly increased with increasing the content of PCL. In every polymer, we found single T_m and T_c , which implies the complete mixing of all the segments within the copolymer.³⁰

Determination of CMC

Different methods have been used to prepare polymeric nanoparticles, for example, direct dissolution, solvent evaporation/film formation, dialysis, and cosolvent evaporation.^{31,32} Selection of any methods depends on factors such as particle size requirement, thermal and chemical stability of the active agent, reproducibility of the release kinetic profiles, and residual toxicity associated with the final product. In the present study, we have selected cosolvent evaporation technique (acetonitrile/water system) for the purpose, as organic solvent of this system can be easily removed at room temperature.⁷ Stability of the nanoparticles was increased with the fraction of PCL. Although semicrystalline nature of PCL enables the penetration of the water molecules in the system and leads the destabilization of nanoparticles, hydrophilic brush provides a polymeric net around the core thereby prevents it from possible corrosion. The location of hydrophobic segment at this stage is well characterized by fluorescence spectra using pyrene as a fluorescence probe.^{7,11} Pyrene was selected as probe to investigate the self-aggregation behavior of the polymer in an aqueous environment. When exposed to a polymeric micelle aqueous solution, pyrene molecules preferably participated in the hydrophobic microdomains of the micelles rather than the aqueous phase. Figure 4 shows the typical fluorescence spectra of pyrene in aqueous medium. At low concentrations, there were low or negligible changes in fluorescence intensity and a shift of (0, 0) band at 328 nm. As the concentration of the micelles increased, a remarkable increase of the total fluorescence intensity and a red shift of the (0, 0) band from 328 to 330 nm were observed. Further the existence of PCL core has been demonstrated by ¹H NMR of MPCL in D₂O, which shows only the

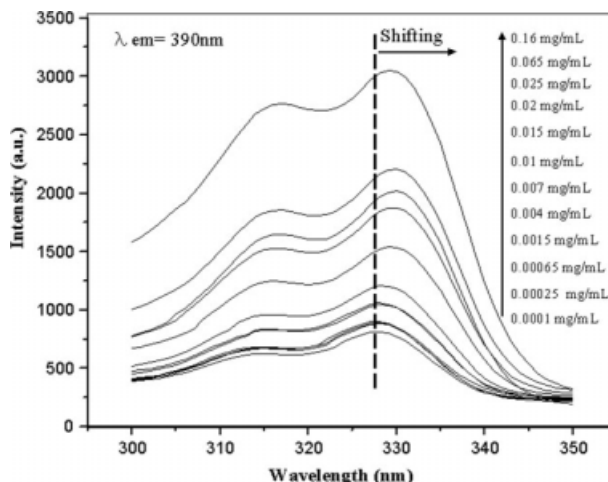


Figure 4 Excitation spectra of pyrene for sample MPCL10 as a function of copolymer concentration.

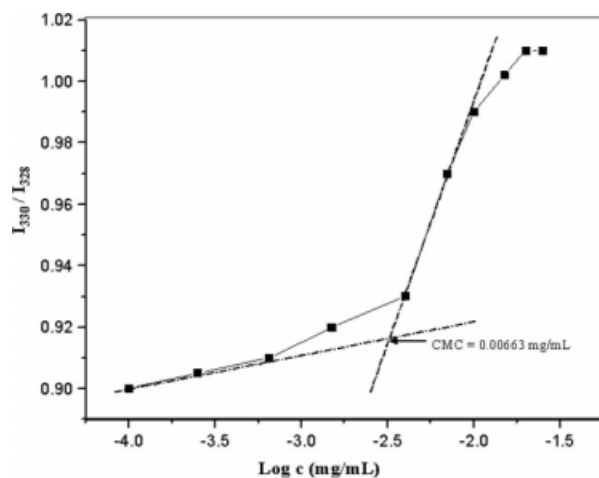


Figure 5 Excitation spectra of pyrene for MPCL10, as a function of copolymer concentration. Intensity ratio (I_{330}/I_{328}) from pyrene ($6 \times 10^{-7} M$) excitation spectra (at a constant $\lambda_{em} = 390$ nm) versus nanoparticles concentration (log C).

resonance corresponds to MPEG citrate but not from PCL moiety (Figure not shown). Figure 5 shows the intensity ratio (I_{330}/I_{328}) of pyrene excitation spectra versus the logarithm of MPCL brush copolymers. On the basis of intensity ratio, the CMC values of the polymers were calculated by the crossover points at low concentration ranges.¹⁹ The CMC values of the copolymers ranged from 19 to 3.1 mg/L as mentioned in Table II. These values obtained from pyrene emission spectra showed similar trends (data not shown). As demonstrated in Table II, the longer the PCL blocks lower the CMC value, exactly as it does in case of diblock copolymers.³³ The brush-like copolymer having a higher surface area provides more rigid or compact hydrophobic core in self-

aggregates with polarization. The result indicates that the formation of nanoparticles is facilitated by the hydrophobicity of the polymer.

Morphology and conformation of MPCL micelles

Micelles developed from highly branched amphiphilic copolymers are associated with a large number of “tunable” surface groups and an interior. This stability study of the particles prepared in PBS reveals that particles hold promise in delivery system. Atomic force microscopy (AFM) observations (Fig. 6) revealed that most of the particles from all the samples were discrete, smooth, regular, and close to sphericity in morphology. Generally, for amphiphilic block copolymer micelles, increasing the length ratio of the hydrophobic block to the hydrophilic, one would expect the increase in the micelle size.²⁶ Two types of micelles were observed in AFM study in aqueous solution: big ones of 60–90 nm [Fig. 6(A)] and small particles with 8–10 nm [Fig. 6(B)].

Typical TEM images also support the two kinds of particles as portrayed in Figure 7. Apparently, all the brush polymer samples aggregate into spherical micelles with two size distributions in water. The smaller ones with a diameter of about 8–10 nm [Fig. 7(A)] are considered as the unimolecular micelles according to the molecular conformations of MPCL, and the larger ones of about 60–90 nm [Fig. 7(B,D)] should be the multimolecular micelles. The formation of larger micelles (secondary micelles) might be due to the further aggregation of smaller micelles (primary micelles). Dynamic light scattering (DLS) study also proved the coexistence of particles with hydrodynamic dimensions of around 118 and 178

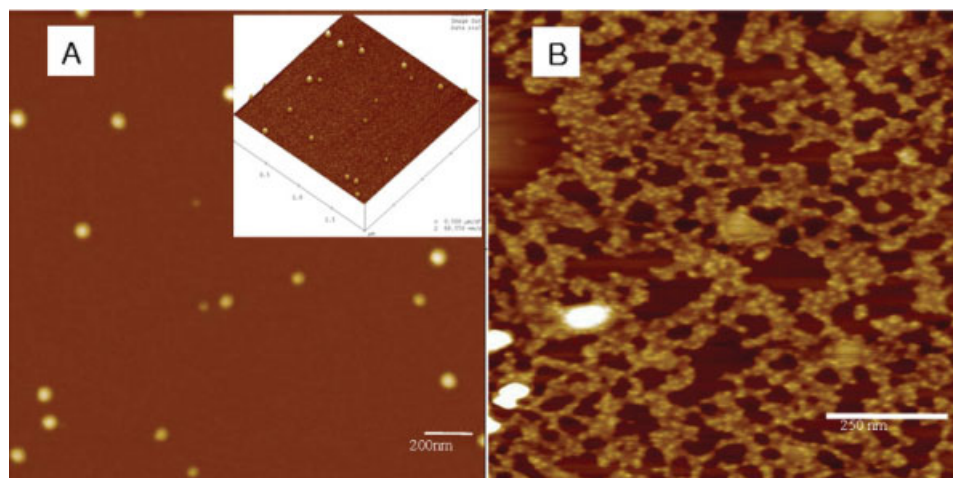


Figure 6 AFM images of MPCL10 nanoparticles: (A) in triple distilled water (inset 3D images), (B) frog egg shaped aggregation of particles (in concentration near to CMC). Two types of nanoparticles have been imaged by AFM: 8–10 nm and 60–90 nm. [Color figure can be viewed in the online issue, which is available at www.interscience.wiley.com.]

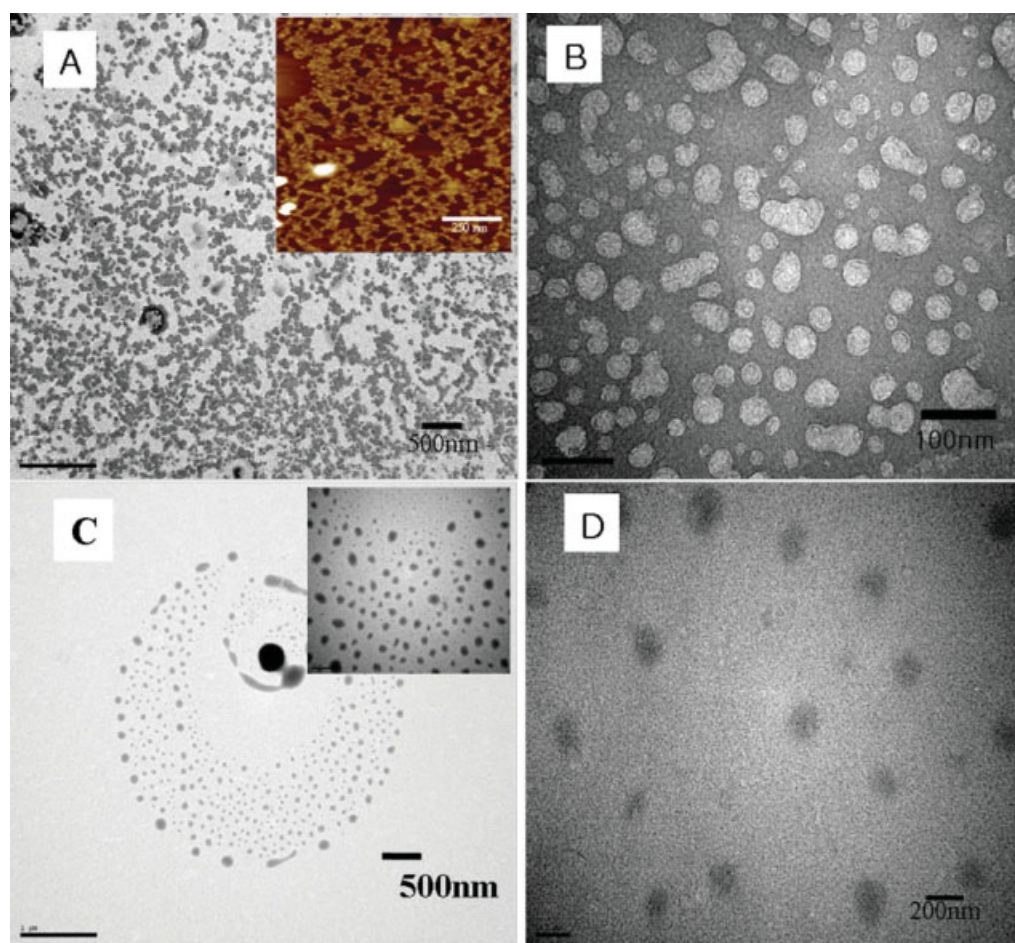
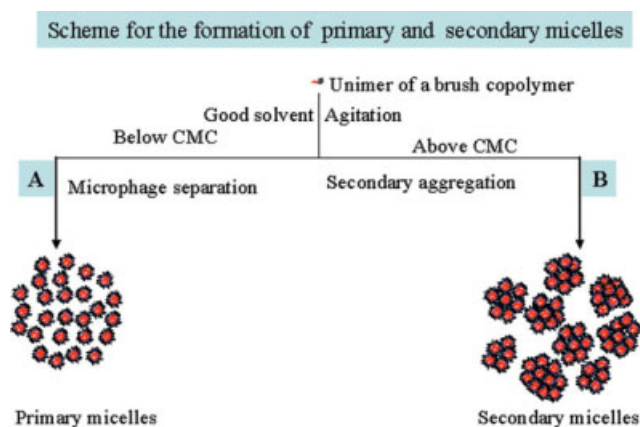


Figure 7 TEM image of MPCL nanoparticles: (A) particles in the phase of aggregation (inset is the AFM images of same particles), (B) formation of secondary particles without staining, (C) larger particles are away from the center of micellar cage (inset shows the high magnified image), and (D) larger particles staining with phosphotungstic acid. Formation of secondary particles with frog egg shaped arrangement possibly because of hydrogen bonding and hydrophobic interaction among the primary micelles. [Color figure can be viewed in the online issue, which is available at www.interscience.wiley.com.]

nm in the aqueous solutions of MPCL copolymer (Table II). Furthermore, the stability of the particles was measured by incubating particles at 37°C in PBS at physiological condition. Herein, a question naturally occurred: what is the driving force for the aggregation of primary micelles? To answer the question, it is useful to observe the molecular structure of MPCL. Interchain overlapping and entangling of MPEG-citrate units might happen during self-assembly, which drives the aggregation of the unimolecular micelles. Such an interchain interaction is probably related with the hydrogen bonding of the hydroxyl groups at the terminal of PCL and hydrophobic interaction among the methylene and methyl groups ($-\text{CH}_3$ and $-\text{CH}_2$) of MPEG units and methylene ($-\text{CH}_2$) groups of PCL chain. In fact, Jerome and coworkers have also found the existence of weak “hydrophobic interaction” between the poly(2-(*N,N*-dimethylaminoethyl methacrylate)) (PDMEMA) chains at room temperature.^{24,34} On the basis of the aforementioned results,



Scheme 2 (A) Formation of primary micelles by microphage separation; (B) formation of large multi molecular (secondary) micelles by the secondary aggregation of primary micelles. The hydrophilic block is in black and hydrophobic block is in red. [Color figure can be viewed in the online issue, which is available at www.interscience.wiley.com.]

we can put forward the self-assembly mechanism of the large multimolecular micelles from the highly branched brush type of copolymers (Scheme 2). The hyperbranched copolymers stay as the unimolecular micelles near CMC, and above CMC (higher concentration than CMC) they further aggregate together to form the large multimolecular micelles due to hydrophobic interaction and hydrogen bonding as discussed earlier.

CONCLUSIONS

Brush copolymers of MPCL have been synthesized by ROP using hydroxyl group of thermally esterified citrate esters as a macroinitiator and stannous octoate as a catalyst. Self-assembled core-shell micellar structure can provide control over low CMC with the higher stability of the micelles. The hydrodynamic size of the micelle is 118 to 178 nm along with two different sizes of core: primary micelles of 8 to 10 nm and secondary micelle of 60 to 90 nm. Such large micelles might be a kind of multimolecular assemblies formed by the secondary aggregation of unimolecular micelles. This integrated brush-like nanopatform will open many exciting opportunities including the targeted delivery of therapeutic agents particularly as a vehicle for anticancer drugs.

References

1. Mayadunne, R.; Jeffery, T. A.; Moad, J.; Rizzardo, G. E. *Macromolecules* 2003, 36, 1505.
2. Mayadunne, R. T. A.; Moad, G.; Rizzardo, E. *Tetrahedron Lett* 2002, 43, 6811.
3. Rizzardo, E.; Chiefari, J.; Mayadunne, R. T. A.; Moad, G.; Thang, S. H. *Macromol Symp* 2001, 174, 209.
4. Szwarc, M. *Nature (London)* 1956, 178, 1168.
5. Szwarc, M.; Levy, M.; Milkovich, R. M. *J Am Chem Soc* 1956, 78, 2656.
6. Ben-Shabat, S.; Kumar, N.; Domb, A. J. *Macromol Biosci* 2006, 6, 1019.
7. Kim, M. S.; Seo, S. K.; Hyun, H.; Khang, G.; Cho, S. H.; Lee, H. B. *J Appl Polym Sci* 2006, 102, 1561.
8. Namazi, H.; Adeli, M. *Biomaterials* 2005, 26, 1175.
9. Peracchia, M. T.; Gref, R.; Minamitake, Y.; Domb, A. J.; Lotan, N.; Langer, R. *J Controlled Release* 1997, 46, 223.
10. Lim, Y.; Pei, Y.; Zhang, X.; Gu, Z.; Zhou, Z.; Yuan, W.; Zhou, J. *J Controlled Release* 2001, 71, 203.
11. Gan, Z. H.; Yu, D. H.; Liang, Q. Z.; Jing, X. B. *Polymer* 1999, 40, 2859.
12. Masahiko, O. *Prog Polym Sci* 2002, 27, 87.
13. Jeong, B. M.; Bae, Y. H.; Lee, D. S.; Kim, S. W. *Nature* 1997, 388, 860.
14. Shin, I. G.; Kim, S. Y.; Lee, Y. M.; Chu, C. S.; Sung, Y. K. *J Controlled Release* 1998, 51, 1.
15. Herold, C. B.; Keil, K.; Bruns, D. E. *Biochem Pharmacol* 1989, 38, 73.
16. Yen, M. S.; Kuo, S. C. *J Appl Polym Sci* 1998, 67, 1301.
17. Ferruti, P.; Mancin, I.; Ranucci, E.; De, C. F.; Latini, G.; Laus, M. *Biomacromolecules* 2003, 4, 181.
18. Li, S. M.; Chen, X. H.; Gross, R. A.; McCarthy, S. P. *J Mater Sci Mater Med* 2000, 11, 227.
19. Choi, C.; Chae, S. Y.; Kim, T.; Kweon, J. K.; Cho, C. S.; Jang, M.; Nah, J. W. *J Appl Polym Sci* 2006, 99, 3520.
20. Lu, C.; Guo, S.; Zhang, Y.; Yin, M. *Polym Int* 2006, 55, 694.
21. Gref, R.; Minamitake, Y.; Peracchia, M. T.; Domb, A. J.; Trubetskoy, V.; Torchilin, V.; Langer, R. *Adv Drug Deliv Rev* 1995, 16, 215.
22. Yang, J.; Webb, A. R.; Ameer, G. A. *Adv Mater* 2004, 16, 511.
23. Cheung, H. Y.; Lau, K. T.; Lu, T. P.; Hui, D. *Compos B* 2003, 8, 291.
24. Hong, H.; Mai, Y.; Zhou, Y.; Yan, D.; Cui, J. *Macromol Rapid Commun* 2007, 28, 591.
25. Ding, T.; Liu, Q.; Shi, R.; Tian, M.; Yang, J.; Zhang, L. *Polym Degrad Stab* 2006, 91, 733.
26. Hu, Y.; Zhang, L.; Cao, Y.; Ge, H.; Jiang, X.; Yang, C. *Biomacromolecules* 2004, 5, 1756.
27. Luo, D.; Haverstick, K.; Belcheva, N.; Han, E.; Saltzman, W. M. *Macromolecules* 2002, 35, 3456.
28. Yang, Z.; Zhang, W.; Liu, J.; Shi, W. *Colloids Surf B* 2007, 55, 229.
29. Bhattarai, N.; Kim, H. Y.; Lee, D. R. *Polym Degrad Stab* 2002, 78, 423.
30. Bhattarai, N.; Kim, H. Y.; Lee, D. R.; Park, S. *J Polym Int* 2003, 52, 6.
31. Allen, C.; Maysinger, D.; Eisenber, A. *Colloids Surf B* 1999, 16, 3.
32. Nakanishi, T.; Fukushima, S.; Okamoto, K.; Suzuki, M.; Matsu-mura, Y.; Yokoyama, M.; Okano, T.; Sakurai, Y.; Kataoka, K. *J Controlled Release* 2001, 74, 295.
33. Nagasaki, Y.; Okada, T.; Scholz, C.; Iijima, M.; Kato, M.; Kataoka, K. *Macromolecules* 1998, 31, 1473.
34. Gohy, J. F.; Creutz, S.; Garcia, M.; Mahltig, B.; Stamm, M.; Jerome, R. *Macromolecules* 2000, 33, 6378.